 CMC, vol.20, no.2, pp.159-183, 2010

Linear Matching Method for Design Limits in Plasticity

Haofeng Chen[1]

Abstract: In this paper a state-of-the-art numerical method is discussed for the evaluation of the shakedown and ratchet limits for an elastic-perfectly plastic body subjected to cyclic thermal and mechanical load history. The limit load or collapse load, i.e. the load carrying capacity, is also determined as a special case of shakedown analysis. These design limits in plasticity have been solved by characterizing the steady cyclic state using a general cyclic minimum theorem. For a prescribed class of kinematically admissible inelastic strain rate histories, the minimum of the functional for these design limits are found by a programming method, the Linear Matching Method (LMM), which converges to the least upper bound. By ensuring that both equilibrium and compatibility are satisfied at each stage, a direct algorithm has also been derived to determine the lower bound of shakedown and ratchet limit using the best residual stress calculated during the LMM procedure. Three practical examples of the LMM are provided to confirm the efficiency and effectiveness of the method: the behaviour of a complex 3D tubeplate in a typical AGR superheater header, the behaviour of a fiber reinforced metal matrix composite under loading and thermal cycling conditions, and effects of drilling holes on the ratchet limit and crack tip plastic strain range for a centre cracked plate subjected to constant tensile loading and cyclic bending moment.

Keywords: Limit load, Shakedown limit, Ratchet limit, Plastic Strain Range, Linear Matching Method

1 Introduction

Engineering design and integrity assessment of components under the action of cyclic thermal and mechanical loading require the assessment of load histories for which certain types of material failure do not occur [Ainsworth (editor) (2003)]. The plastic failure mechanism of a structure subjected to cyclic loads is known as either a local low-cycle fatigue failure (alternating plasticity) or ratchetting with excessive deformation (incremental plasticity). Hence, guarding against alternating

[1] Department of Mechanical Engineering, University of Strathclyde, Glasgow, G1 1XJ, UK

plasticity or ratchetting is important in any design involving cyclic load condition. When the load history is in excess of alternating plasticity limit but less than a ratchet limit, the amplitude of plastic strain needs to be assessed to provide information concerning fatigue crack initiation due to the low cycle fatigue mechanism. The limit load, or the load carrying capacity, which indicates the maximum load that a structure can withstand to avoid plastic collapse, is another crucial design limit in engineering practice.

The determination of these design limits has attracted the attentions of many researchers. The phenomena of shakedown and ratchetting associated with the steady cyclic response have been researched and modeled extensively by plasticity theorists, materials scientists, mathematicians and engineers. Since closed form solutions of these design limits are very limited due to the complexity of the problem, the numerical approaches play a key role for the assessment of these design limits in plasticity. One approach is to simulate the detailed elastic-plastic response of the structure for a specified cyclic load history, most commonly by the incremental Finite Element Analysis (FEA) [ABAQUS (2007)]. Theoretically this allows the investigation of any type of load cycle, but inevitably involves significant computer effort for complex practical structures. To avoid excessive numerical expense associated with the incremental FEA, a relatively new cyclic analysis method, Direct Cyclic Analysis (DCA) [Nguyen-Tajan, Pommier, Maitournam, Houari, Verger, Du, and Snyman (2003)], has been recently incorporated into Abaqus to evaluate the stabilized cyclic behaviour directly, using a modified Newton method in conjunction with a Fourier representation of the solution and the residual vector. However, both the incremental FEA and DCA do not predict shakedown or ratchet limits directly. It can only be used to show whether elastic shakedown, plastic shakedown or ratchetting occurs. To determine the shakedown and ratchet limits, a significant number of trial-and-error processes for the different load levels are required to establish the boundary between shakedown and non-shakedown behaviors, which are very time consuming and impractical for the industrial application. In order for the DCA to identify the shakedown and ratchet limit boundary effectively, the DCA must provide accurate cyclic stress strain solutions when the applied load condition is close to the boundary. However, due to the characteristic of DCA and the inevitable numerical error due to the approximation and convergence problem, the DCA may be not capable of identifying unambiguously the shakedown and ratchet limit boundary [Carter (2005)]. The designer ideally requires direct shakedown and ratchetting analysis method that can be applied to complex 3D geometry under complex loading, does not require unrealistic computing facilities and unambiguously specifies these design limits.

For the shakedown and limit analysis, the primary emphasis in the literature has

been on the use of direct methods, which directly address the shakedown limit and limit load required in a design situation, using both the upper and lower bounding theorems [Koiter (1960); Melan (1933)]. Such methods include mathematical programming methods [Maier (1977); Staat and Heitzer (2001); Chen, Liu and Cen (2008)], the reduced modulus method [Marriott (1998)], the generalized local stress strain R-node method [Seshadri (1995)], the elastic compensation method (ECM) [Mackenzie, Boyle and Hamilton (2000)] and the linear matching method (LMM) [Ponter and Chen (2001); Chen and Ponter (2001, 2010); Chen (2010)]. The LMM originates from the reduced modulus method, R-node method and elastic compensation method, but is distinguished from these methods by ensuring that the equilibrium and compatibility are satisfied at each stage. Among these direct methods, the LMM is counted to be the method most amendable to practical engineering applications involving complicated thermomechanical load history. The LMM has been extensively applied to a range of problems [Chen, Ponter and Ainsworth (2006); Chen and Ponter (2005)], through various adaptations, extended to the calculation required for the UK assessment procedure R5 [Ainsworth (editor) (2003)] for the high temperature response of structures. The LMM describes non-linear inelastic material behaviour by linear solutions where the material coefficients vary both spatially and in time, which makes the method particularly flexible. The LMM has been regarded as an efficient and effective upper bound programming method for which, in many circumstances, strict convergence proofs may be constructed. In the past two years, the LMM has been further developed to account for the lower bound shakedown and ratchets limits, and investigate more complicated cyclic problems.

In this paper, the fundamentals of these methods for design limit in plasticity are readdressed with three objectives in mind. The first is to provide a more general and unified LMM approach for wider class of problems and potential procedures for both upper and lower bound design limits. The second is to investigate and improve the convergence issues in the iterative approach. The third objective is to verify the efficiency and effective of the LMM on the assessment of design limits in plasticity by applying it to three distinctive practical problems.

With extensions to high temperature creep, the LMM has been applied to all stages of the UK's life assessment method R5 [Chen, Ponter and Ainsworth (2006)], for the high temperature response of structures, including the evaluation of the high temperature creep. In this paper, we confine ourselves to cyclic problems where creep is not an issue and give examples from three contrasting areas of application, the behaviour of a complex 3D tubeplate in a typical AGR superheater header, the behaviour of a fiber reinforced metal matrix composite under loading and thermal cycling conditions, and effects of drilling holes on the ratchet limit and crack tip plastic strain range for a centre cracked plate subjected to constant tensile loading

and cyclic bending moment.

In the following sections, a general cyclic minimum theorem for perfect plasticity and the application of the LMM for a particular class of problems for the design limits in plasticity will be described. This is followed by the discussion of convergence and the application of three practical examples with numerical verifications of the proposed methods.

2 Cyclic behaviour

2.1 General cyclic problem

Consider a body with volume V and surface S, where the material is isotropic, elastic-plastic and satisfies the von Mises yield condition. A cyclic history of temperature $\lambda\theta(x,t)$ occurs within volume V. A cyclic load history $\lambda P(x,t)$ is applied over part of S, namely S_T. Here λ denotes a scalar load parameter. On the remainder of S, namely S_u, zero displacements are maintained. Both load and temperature histories have the same cycle time Δt and, in the following, we are concerned with the behaviour of the body in a typical cycle $0 \leq t \leq \Delta t$ in a cycle state. For the problem defined above the stresses and strain rates will asymptote to a cyclic state where;

$$\sigma_{ij}(t) = \sigma_{ij}(t+\Delta t), \quad \dot{\varepsilon}_{ij}(t) = \dot{\varepsilon}_{ij}(t+\Delta t) \tag{1}$$

This arbitrary asymptotic cyclic history may be expressed in terms of three components, the elastic solution, a transient solution accumulated up to the beginning of the cycle and a residual solution that represents the remaining changes within the cycle. The linear elastic stress solution is denoted by $\lambda\hat{\sigma}_{ij}$. The general form of the stress solution is given by

$$\sigma_{ij}(x,t) = \lambda\hat{\sigma}_{ij}(x,t) + \bar{\rho}_{ij}(x) + \rho^r_{ij}(x,t) \tag{2}$$

where $\bar{\rho}_{ij}$ denotes a constant residual stress field in equilibrium with zero surface traction on S_T and corresponds to the residual state of stress at the beginning and end of the cycle. The history ρ^r_{ij} is the change in the residual stress during the cycle and satisfies;

$$\rho^r_{ij}(x,0) = \rho^r_{ij}(x,\Delta t) \tag{3}$$

It is worth noting that the arguments in this section do not explicitly call on the properties of perfect plasticity and are therefore common to all cyclic states associated with inelastic material behaviour.

2.2 Description of design limits in plasticity

Assuming a strictly convex yield condition, which includes the von Mises yield condition in deviatoric stress space;

$$f(\sigma_{ij}) \leq 0 \tag{4}$$

If we define λ^E, λ^S, λ^R and λ^C as the elastic limit multiplier, shakedown limit multiplier, ratchet limit multiplier and collapse load multiplier respectively, then the five major mechanisms including elasticity, shakedown, reverse plasticity, ratchetting and plastic collapse can be described as follows:

E – Elastic region - $0 \leq \lambda \leq \lambda^E$, where $f(\lambda \hat{\sigma}_{ij}) \leq 0$ throughout V.

S – Shakedown - $\lambda^E \leq \lambda \leq \lambda^S$, where $f(\lambda \hat{\sigma}_{ij} + \bar{\rho}_{ij}) \leq 0$, $\bar{\rho}_{ij}$ is a constant residual stress field and plastic strain rate history $\dot{\varepsilon}_{ij}^{pr} = 0$.

P – Reverse or Alternating Plasticity - $\lambda^S \leq \lambda \leq \lambda^R$, where $f(\lambda \hat{\sigma}_{ij} + \bar{\rho}_{ij} + \rho_{ij}^r) \leq 0$, and $\rho_{ij}^r(t)$ is a changing residual stress field, derived from a non-zero plastic strain rate history $\dot{\varepsilon}_{ij}^{pr}$ that satisfies the *zero growth* condition $\int_0^{\Delta t} \dot{\varepsilon}_{ij}^{pr} dt = 0$ everywhere in V.

R – Ratchetting or Incremental plastic collapse - $\lambda^R \leq \lambda \leq \lambda^C$, where $f(\lambda \hat{\sigma}_{ij} + \bar{\rho}_{ij} + \rho_{ij}^r) \leq 0$, and $\rho_{ij}^r(t)$ is a changing residual stress field, derived from a plastic strain rate history $\dot{\varepsilon}_{ij}^{pr}$ that satisfies the *growth* condition $\int_0^{\Delta t} \dot{\varepsilon}_{ij}^{pr} dt = \Delta\varepsilon_{ij}^{pr}$ where $\Delta\varepsilon_{ij}^{pr}$ is a compatible accumulated strain giving rise to non-zero displacement increment Δu_i^{pr}.

C –Plastic collapse - $\lambda^C \leq \lambda$, where $\Delta\varepsilon_{ij}^{pr}$ is compatible with $\Delta u_i^{pr} \neq 0$ at *an instant* during the cycle. The corresponding limit load or plastic collapse load is calculated in this paper as a special case of shakedown analysis, where the number of load instants reduces to 1, i.e. from cyclic loading to monotonic loading.

3 Minimization processes of the linear matching method

The strategy of locating each of above critical limits consists of defining an appropriate class of kinematically admissible strain rate histories $\dot{\varepsilon}_{ij}^c$ then solving a corresponding minimizing process for $I(\dot{\varepsilon}_{ij}^c, \lambda)$ by considering the incremental form;

$$I(\dot{\varepsilon}_{ij}^c, \lambda) = \sum_{n=1}^{N} I^n \tag{5a}$$

$$I^n(\Delta\varepsilon_{ij}^n, \lambda) = \int_V \left\{ \sigma_{ij}^n \Delta\varepsilon_{ij}^n - (\lambda \hat{\sigma}_{ij}(t_n) + \rho_{ij}(t_n) + \bar{\rho}_{ij}) \Delta\varepsilon_{ij}^n \right\} dV \tag{5b}$$

$$\rho_{ij}(t_n) = \sum_{l=1}^{n} \Delta\rho_{ij}(t_l) \tag{5c}$$

where $\dot{\varepsilon}^c_{ij}$ is replaced by a sequence of increments of strain $\Delta\varepsilon^n_{ij}$ occurring at a sequence of N times t_n, n=1 to N, during the cycle. In this section, the linear matching processes for minimization of $I(\dot{\varepsilon}^c_{ij}, \lambda)$ are summarized for both the shakedown and ratchet limits.

3.1 Global minimization for shakedown limit

The global minimization of $I(\dot{\varepsilon}^c_{ij}, \lambda)$ makes use of the compatibility of the sum of the increments of plastic strain over the cycle. When a set of increments $\Delta\varepsilon^{nk}_{ij}$ at kth iteration are assumed known, a linear material can be defined so that linear shear modulus $\bar{\mu}^{nk}$ ensures that the resulting deviatoric stress is at yield, i.e.

$$2/3\bar{\mu}^{nk}\bar{\varepsilon}(\Delta\varepsilon^{nk}_{ij}) = \sigma_y \tag{6}$$

where $\bar{\varepsilon}$ denotes the von Mises effective strain.

For shakedown problems, the changing component of residual stress $\rho^r_{ij} = 0$. Hence, the cyclic stress history for shakedown problem is given by

$$\sigma_{ij}(x,t) = \lambda\,\hat{\sigma}_{ij}(x,t) + \bar{\rho}_{ij}(x) \tag{7}$$

A set of linear incremental relationships are then defined by

$$\Delta\varepsilon^{n(k+1)\prime}_{ij} = \frac{1}{2\bar{\mu}^{nk}}[\lambda\,\hat{\sigma}_{ij}(t_n)' + \bar{\rho}^{k+1\prime}_{ij}], \quad \Delta\varepsilon^{n(k+1)}_{kk} = 0 \tag{8}$$

where the upper 'dash' refers to deviatoric components. Summing over the cycle produces a relationship between the compatible strain $\Delta\varepsilon^{(k+1)}_{ij} = \sum_n \Delta\varepsilon^{n(k+1)}_{ij}$ and the constant residual stress $\bar{\rho}^{k+1}_{ij}$ with an initial stress state;

$$\Delta\varepsilon^{(k+1)\prime}_{ij} = \frac{1}{2\bar{\mu}^k}\left(\sigma^{initial\prime}_{ij} + \bar{\rho}^{k+1\prime}_{ij}\right), \quad \Delta\varepsilon^{(k+1)}_{kk} = 0 \tag{9a}$$

where $\frac{1}{\bar{\mu}^k} = \sum_n \frac{1}{\bar{\mu}^{nk}}$ and

$$\sigma^{initial}_{ij} = \bar{\mu}^k \sum_n \frac{\lambda\,\hat{\sigma}_{ij}(t_n)}{\bar{\mu}^{nk}} \tag{9b}$$

The solution of the continuum problem corresponding to equation (9) has the property that $I(\Delta\varepsilon^{(k+1)}_{ij}, \lambda) \le I(\Delta\varepsilon^k_{ij}, \lambda)$, which is proved by [Ponter and Chen (2001)].

3.2 Dual minimization process for ratchet analysis

We consider a structure subjected to a general cyclic load condition, which can be decomposed into cyclic and constant components, i.e. $\hat{\sigma}_{ij}(x,t) = \hat{\sigma}^{\Delta}_{ij}(x,t) + \lambda \hat{\sigma}^{\overline{F}}_{ij}(x)$. The calculation of the ratchet limit includes dual minimization processes, the first an incremental minimization for the evaluation of a cyclic history of residual stresses and plastic strain range in a stable cycle and the second a global minimization for the ratchet limit due to an extra constant load. By decoupling the evaluation of the changing residual stress and the constant residual stress in (5), the entire numerical procedure of ratchet analysis includes two steps [Chen and Ponter (2010)]. The first step is to calculate the history of the changing residual stress associated with the applied cyclic load $\hat{\sigma}^{\Delta}_{ij}(x,t)$ and the corresponding plastic strain ranges for the low cycle fatigue assessment. The second step is to locate the ratchet limit due to the extra constant load $\lambda \hat{\sigma}^{\overline{F}}_{ij}(x)$ as a conventional shakedown analysis where a constant residual stress is evaluated by global minimization (section 3.1) and the elastic stress history is augmented by the changes in residual stress calculated in the first step.

The global minimization process for step 2 of ratchet analysis is as same as the global minimization for shakedown limit in section 3.1. Next a distinct minimization process – incremental minimization is summarized for step 1 of ratchet analysis to evaluate the changing residual stress ρ^{r}_{ij} and the associated plastic strain range corresponding to the cyclic component of the elastic stress $\hat{\sigma}^{\Delta}_{ij}$.

3.2.1 Incremental minimization for the varying residual stress field and plastic strain range

The incremental minimization of $I^{n}(\Delta\varepsilon^{n}_{ij}, \lambda)$ assumes the prior history of the residual stress is known and compatibility of the total elastic and plastic strain in the increment is used.

With an initial estimate of $\Delta\varepsilon^{n}_{ij} = \Delta\varepsilon^{nk}_{ij}$, a linear modulus is defined by linear matching $\sigma_y = 2/3\bar{\mu}^{nk}\bar{\varepsilon}(\Delta\varepsilon^{nk}_{ij})$, where the von Mises yield stress σ_y could be either constant or temperature-dependant.

An incremental linear equation is then defined;

$$\Delta\varepsilon^{Tn(k+1)'}_{ij} = \frac{1}{2\mu}\Delta\rho^{n(k+1)'}_{ij} + \Delta\varepsilon^{n(k+1)'}_{ij} \tag{10a}$$

$$\Delta\varepsilon^{Tn(k+1)}_{kk} = \frac{1}{3K}\Delta\rho^{n(k+1)}_{kk} \tag{10b}$$

$$\Delta\varepsilon^{n(k+1)'}_{ij} = \frac{1}{2\bar{\mu}^{nk}}\left\{\hat{\sigma}^{\Delta}_{ij}(t_n) + \rho_{ij}(t_{n-1}) + \Delta\rho^{n(k+1)}_{ij}\right\}' \tag{10c}$$

where the prior history of the residual stress is known, i.e. $\rho_{ij}(t_{n-1}) = \rho_{ij}(t_0) + \Delta\rho_{ij}^1 + \Delta\rho_{ij}^2 + ... + \Delta\rho_{ij}^{n-1}$,

$$\rho_{ij}(t_0) = \bar{\rho}_{ij}^0 \tag{11}$$

The entire iterative procedure requires a number of cycles, where each cycle contains N iterations associated with N load instances. The first iteration is to evaluate the changing residual stress $\Delta\rho_{ij}^1$ associated with the elastic solution $\hat{\sigma}_{ij}^{\Delta}(t_1)$ at the first load instance. Define $\Delta\rho_{ijm}^n$ as the evaluated changing residual stress for *nth* load instance at *mth* cycle of iterations, where n=1,2,...N and m=1,2,...M. At each iteration, the above changing residual stress $\Delta\rho_{ijm}^n$ is calculated. When the convergence occurs at the *Mth* cycle of iterations, the summation of changing residual stresses at N time points must approach to zero ($\sum_{n=1}^{N} \Delta\rho_{ijM}^n = 0$) due to the stable cyclic response. Hence the constant residual stress $\rho_{ij}(t_0) = \bar{\rho}_{ij}^0$ over the cycle can also be determined by

$$\bar{\rho}_{ij}^0 = \sum_{n=1}^{N} \Delta\rho_{ij1}^n + \sum_{n=1}^{N} \Delta\rho_{ij2}^n + \cdots + \sum_{n=1}^{N} \Delta\rho_{ijM}^n \tag{12}$$

The corresponding plastic strain magnitude occurring at time t_n is calculated by

$$\Delta\varepsilon_{ij}^P(t_n) = \frac{1}{2\bar{\mu}^n}\left(\hat{\sigma}'^{\Delta}_{ij}(t_n) + \rho'_{ij}(t_n)\right) \tag{13}$$

where $\bar{\mu}^n$ is the iterative shear modulus and $\rho_{ij}(t_n)$ is the converged accumulated residual stress at the time instant t_n, i.e.

$$\rho_{ij}(t_n) = \bar{\rho}_{ij}^0 + \sum_{k=1}^{n} \Delta\rho_{ijM}^k \tag{14}$$

4 Evaluation of upper bound limits

4.1 Upper bound shakedown limit

Combining $0 \le I(\Delta\varepsilon_{ij}^{(k+1)}, \lambda) \le I(\Delta\varepsilon_{ij}^k, \lambda)$ and Eq. 5, with ρ_{ij} and $\bar{\rho}_{ij}$ eliminated and $\lambda = \lambda_S$, following inequality exists;

$$I(\Delta\varepsilon_{ij}, \lambda^S) = \int_V \sum_{n=1}^{N} \left\{\sigma_{ij}^n \Delta\varepsilon_{ij}^n - \lambda^S \hat{\sigma}_{ij}(t_n)\Delta\varepsilon_{ij}^n\right\} dV \ge 0 \tag{15}$$

$$i.e. \quad \lambda^S \leq \frac{\int_V \left(\sum_{n=1}^{N} \sigma_{ij}^n \Delta\varepsilon_{ij}^n \right) dV}{\int_V \left(\sum_{n=1}^{N} \hat{\sigma}_{ij}(t_n) \Delta\varepsilon_{ij}^n \right) dV} = \frac{\int_V \left(\sigma_y \sum_{n=1}^{N} \bar{\varepsilon}(\Delta\varepsilon_{ij}^n) \right) dV}{\int_V \left(\sum_{n=1}^{N} \hat{\sigma}_{ij}(t_n) \Delta\varepsilon_{ij}^n \right) dV} = \lambda_{UB}^S \tag{16}$$

Eq. 16 provides a monotonically reducing sequence of upper bound to the shakedown limit, i.e. $\lambda_{UB}^{S(k+1)} \leq \lambda_{UB}^{S(k)}$. It is worth noting that a limit load can be calculated by Eq.16 as a special case of the shakedown analysis, where the cyclic load condition reduces to monotonic load condition, i.e. N=1.

4.2 Upper bound ratchet limit

As described in [Chen and Ponter (2010)], once the history of the residual stress field $\rho_{ij}(t_n)$ associated with the cyclic component of the load history has been calculated by an incremental minimization process (section 3.2.1), the numerical technique for the ratchet limit can be accommodated within the existing methods of shakedown analysis where the linear elastic solution is augmented by the changing residual stress field, i.e.

$$\hat{\sigma}_{ij} = \lambda \hat{\sigma}_{ij}^{\bar{F}} + \hat{\sigma}_{ij}^{\Delta}(x,t) + \rho_{ij}(x,t) \tag{17}$$

For the von Mises yield condition and the associated flow rule, an upper bound on the ratchet limit multiplier can be obtained by

$$\lambda_{UB}^R = \frac{\int_V \sum_{n=1}^{N} \sigma_y \bar{\varepsilon} \left(\Delta\varepsilon_{ij}^n \right) dV - \int_V \sum_{n=1}^{N} \left(\hat{\sigma}_{ij}^{\Delta}(t_n) + \rho_{ij}(t_n) \right) \Delta\varepsilon_{ij}^n dV}{\int_V \hat{\sigma}_{ij}^{\bar{F}} \left(\sum_{n=1}^{N} \Delta\varepsilon_{ij}^n \right) dV} \tag{18}$$

which gives the capacity of the body subjected to a predefined cyclic load history $\hat{\sigma}_{ij}^{\Delta}(t_n)$ to withstand an additional constant load $\hat{\sigma}_{ij}^{\bar{F}}$ before ratchetting takes place.

As for the shakedown limit, Eq.18 produces a sequence of monotonically reducing upper bounds λ_{UB}^R, which converge to the least upper bound ratchet limit for the chosen class of displacement fields. It is worth noting that within the LMM the adoption of the yield stress is flexible for both the shakedown and ratchet analyses, i.e. the yield stress of the material can be varied with both time and location. For example, when considering temperature-dependant yield stress, σ_y in Eq. (16) and (18) is then replaced by $\sigma_y(T)$.

5 Evaluation of lower bound limits

Both the constant residual stress $\bar{\rho}_{ij}(x)$ and varying residual stress $\rho_{ij}^r(x,t)$ in Eq.2 for a stabilised load cycle have been calculated by incremental and global mini-

mization processes. Hence, based upon the lower bound theorem [Melan (1933)], a lower bound of shakedown or ratchet limit can be constructed in the same upper bound procedure by maximizing the lower bound load parameter λ_{LB} under the condition where for any potentially active load/temperature path, the stabilised cyclic stresses in Eq.2 nowhere violate the yield condition.

As the upper bound iterative process provides a sequence of residual stress fields, a sequence of lower bound at each iteration can be calculated by scaling the elastic solution so that the cyclic stress everywhere satisfies yield. The lower bound of shakedown limit multiplier can be described as:

$$\lambda_{LB}^{s} = \max\ \lambda_{LB} \tag{19a}$$

$$s.t. \quad f(\lambda_{LB}\hat{\sigma}_{ij}(x,t) + \bar{\rho}_{ij}(x)) \leq 0 \tag{19b}$$

The lower bound of ratchet limit multiplier can be written as:

$$\lambda_{LB}^{R} = \max\ \lambda_{LB} \tag{20a}$$

$$s.t. \quad f(\lambda_{LB}\hat{\sigma}_{ij}^{\bar{F}} + \hat{\sigma}_{ij}^{\Delta}(x,t) + \rho_{ij}(x,t) + \bar{\rho}_{ij}(x)) \leq 0 \tag{20b}$$

6 Convergence considerations

The discussion of sufficient condition for convergence and the strict proof for upper bounds were provided by [Ponter and Engelhardt (2000); Ponter and Chen (2001)]. In summary, the process of obtaining a convergent minimum upper bound limits requires three conditions to be satisfied: 1) The convexity of material yield surface; 2) The class of strain rates and associated strain increments ensures that the minimum upper bound is contained with this class; 3) The class of chosen compatible strain distributions needs to be sufficiently wide to ensure an acceptable upper bound.

The first two conditions can be easily satisfied by an appropriate choice of a class of linear materials. Condition (3) is vital to the implementation of the LMM within a finite element scheme. Within the LMM, the equilibrium of the residual stress field ρ_{ij} relies on the class of displacement field Δu_i from which $\Delta\varepsilon_{ij}$ is derived, i.e. ρ_{ij} is in equilibrium if and only if $\int_V \rho_{ij}\Delta\varepsilon_{ij}dV = 0$. Hence, for a given finite element mesh, the process will converge to the least upper bound associated with the FE mesh and within this class of displacement field Δu_i. However, during the FE implementation, the volume integration is not exact but usually depends upon the Gaussian integration to give an exact integral. Hence a point-wise condition is used to replace above equilibrium condition;

$$\sum_{el}\sum_{k} w_k \rho_{ij}^{k} \Delta\varepsilon_{ij}^{k} = 0 \tag{21}$$

where w_k are the Gaussian weighting factors at the Gauss integration points.

According to the lower and upper bound theorems, the LMM ensures that the maximum lower bound will be less than the least upper bound. However, unlike the strict convergence of the upper bound, the magnitude of lower bound may not always increase monotonically with iterations. But upon convergence, the maximum lower bound will equal to the least upper bound, where by equilibrium condition (Eq.21) the matching condition is applied at Gauss points.

Due to the point-wise condition of equilibrium (Eq.21), whereas the deviation from convergence at a few Gauss points has little effect on the upper bound which is determined by volume integrals, the convergence of the upper bound in terms of a particular number of significant figures may allow some deviation from convergence locally. Hence the convergence of lower bound may be affected significantly as it is determined by single Gauss point. Generally the upper bound converges (monotonically) more quickly than the lower bound and the rate of convergence for lower bound depends upon the characteristic of the problem and also the adopted FE model, such as the complexity of the geometry and boundary conditions, the mesh arrangement, etc. For some cases where the lower bound converges very slowly, the convergence is usually judged entirely in terms of the upper bound. Further investigation of the convergence of the LMM iterative algorithms has been carried out and a separate paper is being prepared for this context.

7 Examples of applications

In this section, three practical examples of the LMM for differing applications are provided to confirm the efficiency and effectiveness of the method; the behaviour of a heat exchanger in a typical AGR superheater header, the shakedown and ratchet analyses of fiber reinforced metal matrix composites subjected to cyclic temperature loads and constant macro stress, and effects of drilling holes on the ratchet limit and crack tip plastic strain range for a centre cracked plate subjected to constant tensile loading and cyclic bending moment.

7.1 A heat exchanger tubeplate subjected to severe cyclic thermal loading and constant operating pressure

Fig. 1 gives a 1/16-th sectional view of a heat exchanger from a power plant. Such exchangers are subjected to particular severe thermal loading, resulting in the possibility of ratchetting or premature failure due to low cycle fatigue.

The tubeplate experiences the most extreme temperature distributions that occur when the superheated steam supply is suddenly disconnected (Boiler Trip) and when the superheated steam supply is reconnected (Boiler Reconnect). At the same

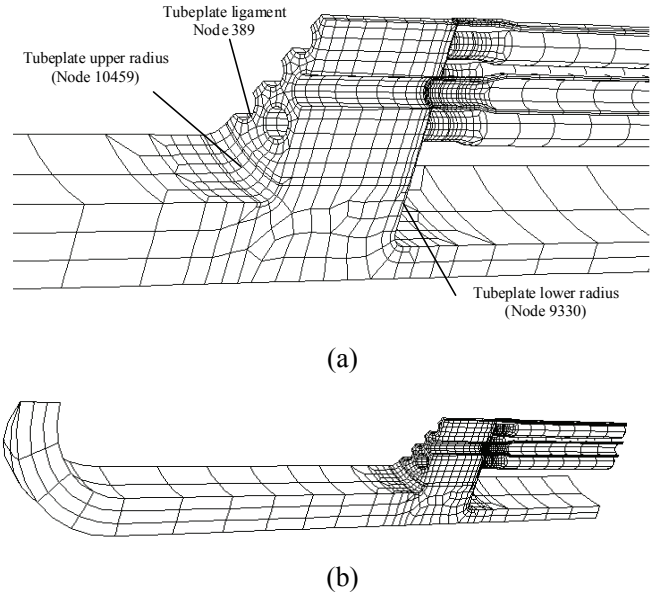

Figure 1: Sectional view of superheater header showing tubeplate features

time there is a varying internal gas and steam pressure. Hence, this load cycle type is selected for the shakedown and ratchet analysis. Other load cycle types with a smaller elastic stress range are expected to be encompassed in terms of cyclic behaviour. Hence, the cyclic loading is defined by the following two extreme loading conditions:

(1) Boiler Trip – The temperature distribution giving rise to the maximum von Mises thermal stress during a boiler trip transient plus the prevailing gas and steam pressure;

(2) Boiler Reconnection – The temperature distribution giving rise to the maximum von Mises thermal stress during a boiler reconnection transient plus the prevailing gas and steam pressures.

The corresponding linear elastic stress histories were evaluated and the maximum variation of effective elastic stress due to the varying temperature distribution and pressure from Boiler Trip to Boiler Reconnection was denoted by $\Delta\hat{\sigma}_{TP}^{BT-RC}$. This linear solution was then scaled and the vertical axis of Fig. 2 $\Delta\hat{\sigma}/\Delta\hat{\sigma}_{TP}^{BT-RC}$ corresponds to differing scaling factors where $\Delta\hat{\sigma}/\Delta\hat{\sigma}_{TP}^{BT-RC} = 1$ corresponds to the

actual history. The horizontal axis $\hat{\sigma}/\hat{\sigma}_P^{SS}$ corresponds to the maximum elastic effective stress for an internal pressure, where $\hat{\sigma}/\hat{\sigma}_P^{SS} = 1$ corresponds to the internal pressure experienced by the heat exchanger in normal operation. Variation of the yield stress with temperature was taken into account as this has a significant effect on the solutions.

Fig. 2 can be subdivided into three regions where shakedown (S), reverse plasticity (P) and ratchetting (R) occurs. The method is also adapted to consider cyclic hardening, which affects the position of the ratchet boundary. Using the known steady state cyclic behaviour for the material (an austenitic stainless steel), the corresponding ratchet boundary is shown in Fig. 2 as a dashed line. This method of representing the behaviour of the structure can be seen to have considerable advantages. The actually loading history, $\Delta\hat{\sigma}/\Delta\hat{\sigma}_{TP}^{BT-RC} = 1$, lies slightly outside the ratchet boundary assuming perfect plasticity. When cycle hardening is taken into account, the load point lies on the ratchet boundary. This characteristic of the problem corresponds very well with the known behaviour of the component.

Not only the location of the load point in relation to the ratchet boundary, but also the plastic strain range concerning the fatigue crack initiation in a low cycle fatigue assessment are of greatest interest, as the load point lies well outside the shakedown region. Fig. 3 presents the calculated maximum plastic strain range with increasing load amplitude. For the perfect plasticity case, the maximum plastic strain range occurs, for lower load values, at the upper radius. For load values in excess of approximately 0.8-0.9, the maximum occurs at the tubeplate ligament (see Fig. 1). For the cyclic hardening model the maximum values always occur at the upper radius. Unlike the slight contribution of the hardening on the ratchet limit, the plastic strain ranges are significantly reduced by adopting the cyclic hardening model. Hence it is important to consider cyclic hardening to calculate this key parameter of the fatigue limit.

A full discussion of the solutions and comparisons with step-by-step solutions for complex constitutive equations are given by [Chen and Ponter (2005)]. This example demonstrates that, for these complex industrial problems, the method is capable of providing solutions that are much more illuminating than conventional analysis.

7.2 Fiber reinforced metal matrix composite subjected to cyclic temperature loads and constant macro stress

This example concerns the behaviour of a metal matrix composite material, which consists of a combination of a ductile matrix metal within which is incorporated, in a regular manner, a ceramic. The ceramic may be in the form of long continuous fibers or particles. Such materials have higher strength, greater stiffness and lower density than the monolithic matrix material and hence are potentially advantageous

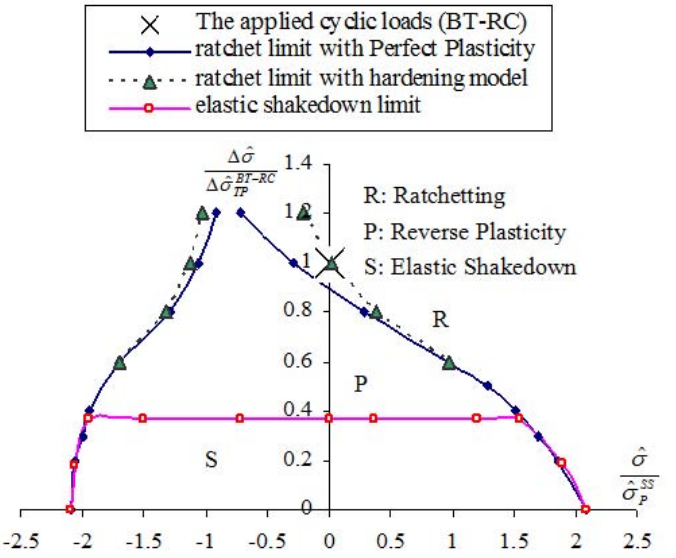

Figure 2: The shakedown limit and ratchet limit interaction curves for heat exchanger tubeplate with cyclic loading condition

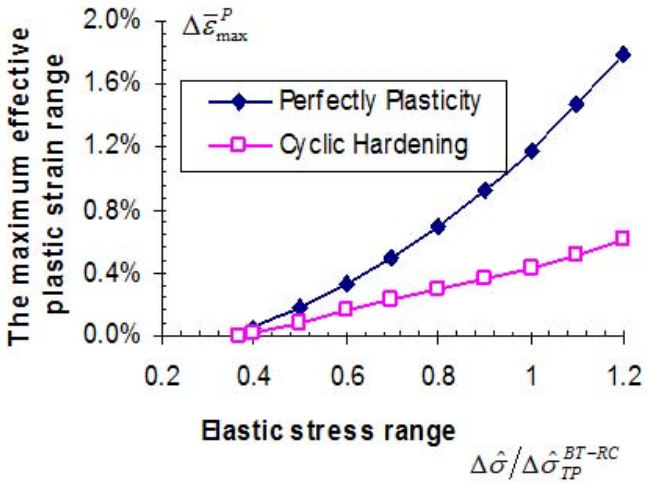

Figure 3: The maxima of the effective plastic strain ranges with different material models over all Gauss integration points

for aerospace applications. However the effect of variable temperature on such materials is potentially difficult to understand. The significantly differing coefficients of thermal expansion between ceramic and metal give rise to micro thermal stresses when the uniform temperature of the material is changed.

We consider an idealized, fiber-reinforced composite that consists of a square array of SiC fibers in an elastic-plastic matrix of Aluminum. The cell which is indicated in Fig. 4a is investigated in a quarter FE model (Fig. 4b) under plain strain condition by both the LMM and Abaqus inelastic step-by-step analysis for the verification of the LMM results. The volume fraction occupied by the ceramic fiber V_f=11%.

A uniaxial macro-stress σ_P is applied in a direction parallel to an edge of the generic cube and maintained constant. The temperature of the composite remains uniform but varies cyclically over a range 0 to $\Delta\theta$. The generic cube is subjected to homogenization boundary conditions so that the surface displacement in a single cube is consistent with that of adjacent, identical cubes.

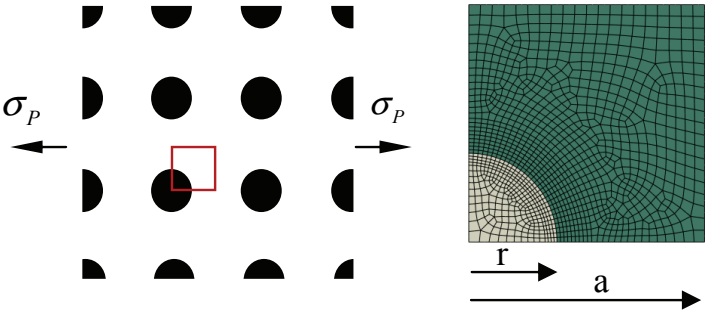

Figure 4: a) Schematic diagram of the fiber reinforced MMC (V_f=11%) as loaded; b) The unit cell used in the FEA

Fig.5 shows lower and upper bound shakedown and ratchet limit interaction diagram where the axis are expressed in non-dimensional variables, σ_p/σ_{p0} and $\Delta\theta/\Delta\theta_0$. Here σ_{p0} equals the yield stress of Aluminum, 30MPa, and $\Delta\theta_0$=50^{o}C. The most noticeable feature of Fig. 5 is the observation that the effective strength of the composite approaches to zero when the variable temperature $\Delta\theta/\Delta\theta_0$ is greater than 0.9. It is also clear from Fig. 5 that for both shakedown and ratchet limits, the LMM produces lower and upper bounds converge very close to each other. This indicates

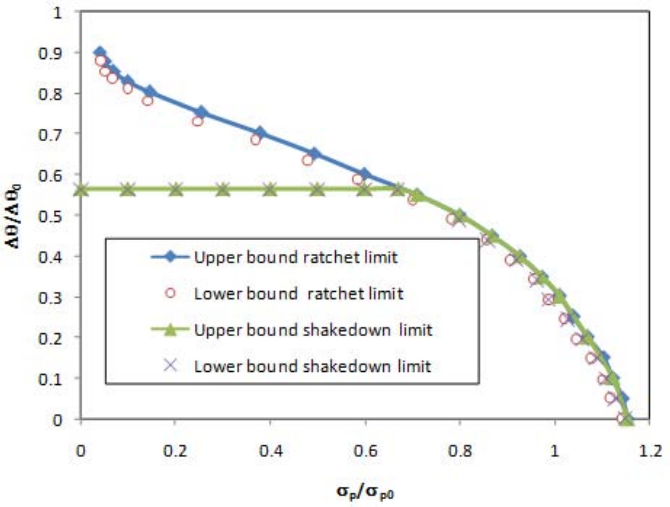

Figure 5: Lower and upper bound shakedown and ratchet limits for fiber-reinforced composite consisting of an Aluminum matrix with SiC fibers where V_f=11%

that the LMM is capable of producing very accurate shakedown and ratchet limits for this type of cyclic problems.

Figs. 6 and 7 present the calculated maximum plastic strain range and ratchetting strain per cycle by both the LMM and Abaqus step-by-step analysis for MMC subjected to varying cyclic thermal loads $\Delta\theta$ and constant σ_p=0 and 8MPa, respectively. The coincidence of LMM and Abaqus step-by-step analysis results in Figs. 6 and 7 confirms the accuracy of the LMM. However, comparing with the LMM, the Abaqus step-by-step analysis involves much more significant computer effort to produce the same results. It is also observed that there is no ratchetting when the uniaxial macro-stress σ_p=0, and however, when σ_p=8MPa, the ratchetting strain occurs when the variable temperature $\Delta\theta/\Delta\theta_0$ is greater than 0.75. The most interesting observation from Figs. 6 and 7 is that the magnitude of maximum plastic strain range concerning the fatigue crack initiation not only depends upon the varying cyclic thermal loads $\Delta\theta$, but is also affected by the constant uniaxial macro-stress σ_p. The mild increase of the plastic strain range due to the existence of the constant uniaxial macro-stress agrees very well with the general experimental observations.

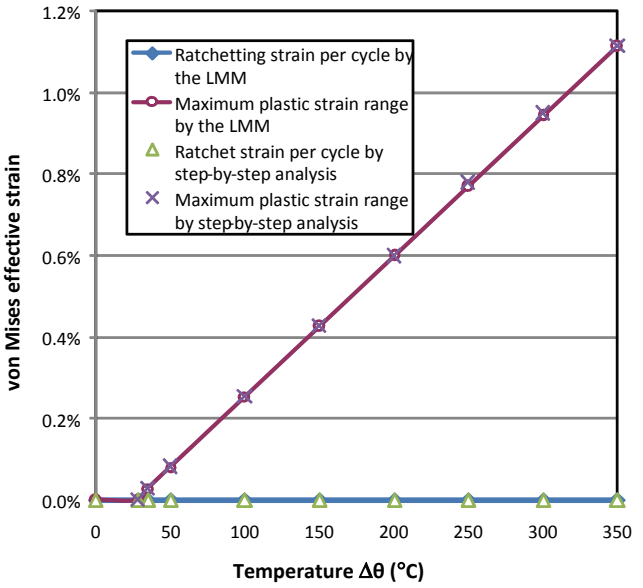

Figure 6: Maximum plastic strain range and ratchetting strain per cycle for MMC subjected to varying cyclic thermal loads $\Delta\theta$ and constant σ_p=0

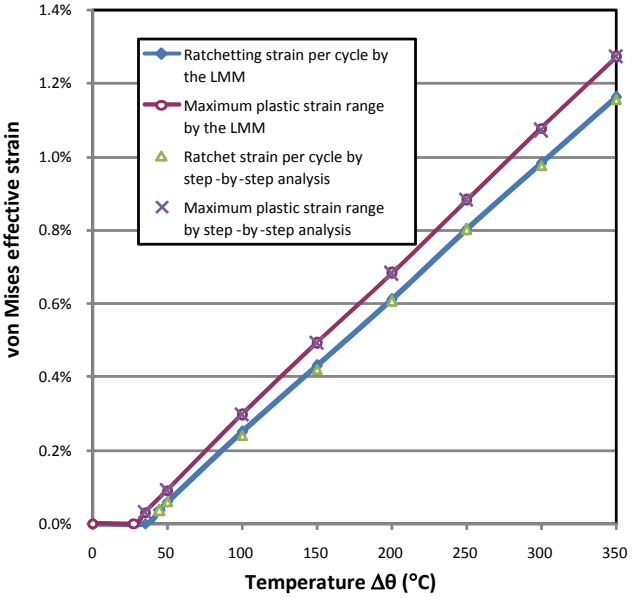

Figure 7: Maximum plastic strain range and ratchetting strain per cycle for MMC subjected to varying cyclic thermal loads $\Delta\theta$ and constant σ_p=8MPa

7.3 Centre cracked plate with circular holes

The final example concerns the effect of circular holes in a centre cracked plate subjected to cyclic bending moment and constant tensile loading on the ratchet limit and crack tip plastic strain range. Drilling holes in front of the crack tip is an effective way to arrest crack growth. However the optimum location and size of the holes need to be researched to produce the smallest crack tip plastic strain range, i.e. the best fatigue crack growth life, and to have the least reduction in ratchet limit.

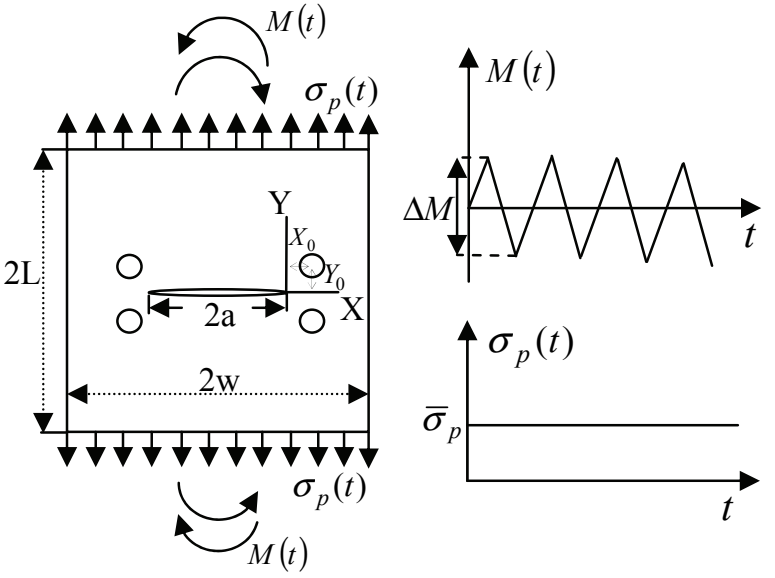

Figure 8: Centre cracked plate with symmetric holes subjected to reversed bending moment range ΔM and constant tension $\bar{\sigma}_p$

The geometrical shape and cyclic loading history of the centre cracked plate with symmetric drilled holes are shown in Fig.8, where the half-crack length a is 500 mm and the ratios W/a and L/a are both 2. The hole locations (X_0, Y_0) are referred to a co-ordinate system X, Y, the origin of which is located at the crack tip. The centre cracked plate is subjected to cyclic reversed bending moment with range ΔM and constant uniaxial tension $\bar{\sigma}_p$. By applying symmetry conditions, a FE half symmetry model was adopted (Fig. 9).

Fig. 10 presents the calculated lower and upper ratchet limit and limit load interaction diagram for the hole location at X/a= -1, Y/a=0.3 and the diameter of hole

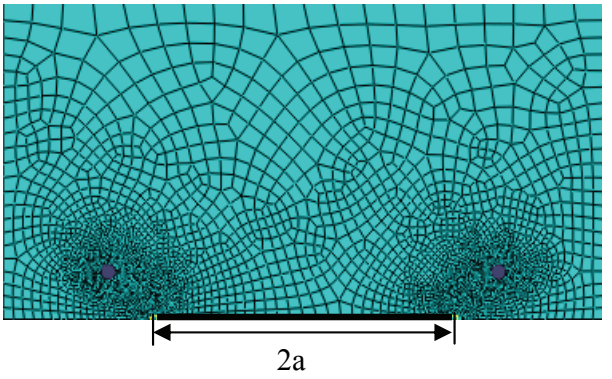

Figure 9: FE half symmetry model for centre cracked plate with symmetric holes

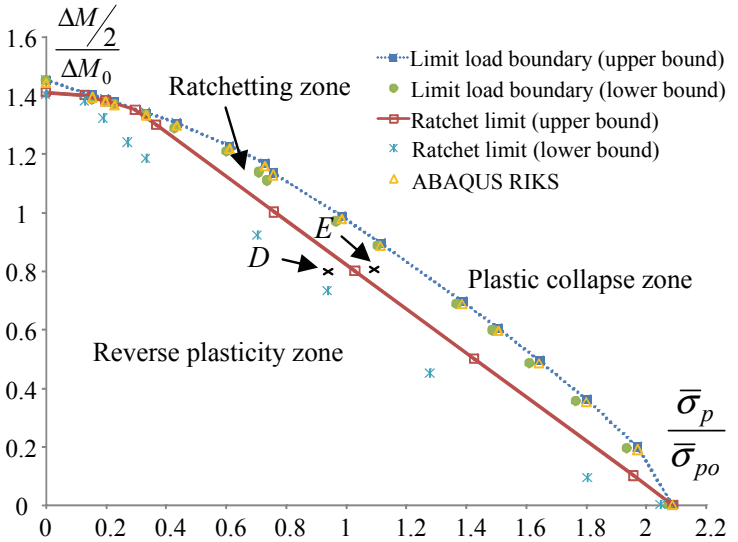

Figure 10: Ratchet limit and limit load interaction curve with hole location at $X/a = -0.1, Y/a = 0.3$ (D=100mm)

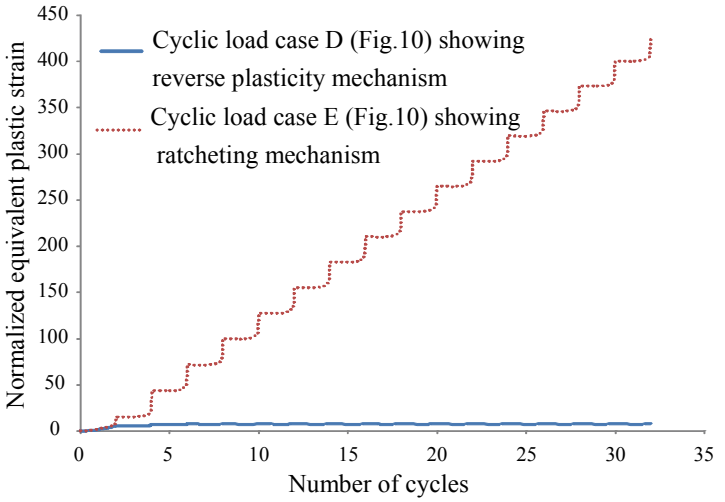

Figure 11: BAQUS verification of the ratchet limit for the cyclic bending moment case using detailed step by step analysis

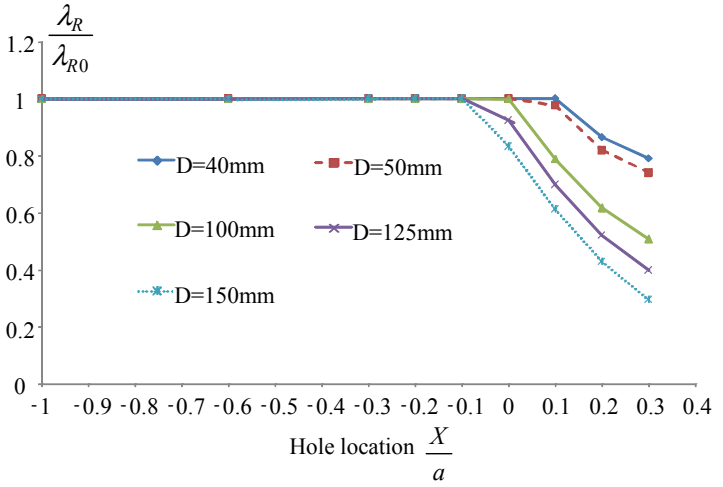

Figure 12: Variation of normalized ratchet limit multiplier with varying horizontal hole location at the fixed vertical location $(Y/a = 0.3)$ and prescribed reversed bending moment $(\Delta M/2)/\Delta M_0 = 1$

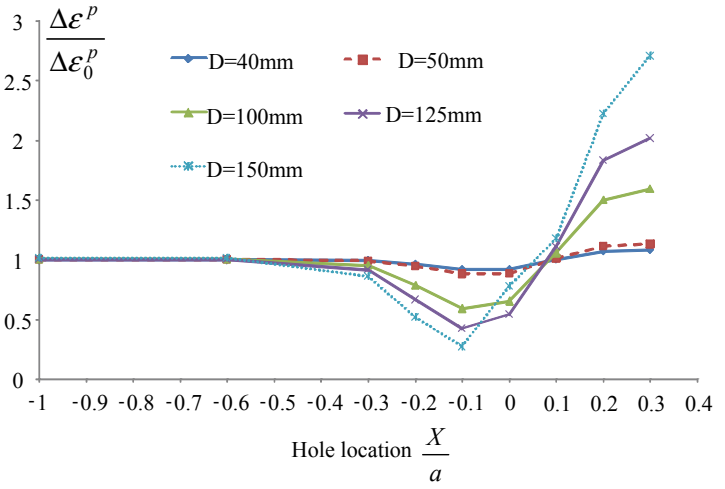

Figure 13: ariation of normalized maximum plastic strain range with varying horizontal hole location at the fixed vertical location ($Y/a = 0.3$) and prescribed reversed bending moment $(\Delta M/2)/\Delta M_0 = 1$

D=100mm, where the applied constant pressure in X-axis is normalized with respect to the reference uniaxial tension $\bar{\sigma}_{po} = 100MPa$, while the amplitude of the reversed bending moment in Y-axis is normalized using the reference bending moment range $\Delta M_0 = 100N \cdot mm$. It can be seen that the ratchet limit and the limit load curves do not coincide, which means that an increase in the loads beyond the ratchet limit will not automatically cause plastic collapse. Any combination of loads which lies between these two boundaries will result in ratchetting. As shown in Fig. 10, the accuracy of the lower and upper bound limit load boundary obtained by the LMM has been verified by ABAQUS RIKS analysis. For the verification of LMM lower and upper bound ratchet limit boundary the cyclic load points D($\Delta M = 1.6\Delta M_0$, $\bar{\sigma}_p = \bar{\sigma}_{p0}$), and E($\Delta M = 1.6\Delta M_0$, $\bar{\sigma}_p = 1.1\bar{\sigma}_{p0}$), which are just below and above the calculated upper bound ratchet limit boundary (Fig.10), respectively, are chosen for the step-by-step analysis in ABAQUS.

Fig. 11 shows the plastic strain history at the crack tip for the cyclic loading D and E calculated by ABAQUS step-by-step analysis. The calculated plastic strain for the load case D settles to a stable cycle after about 5 load cycles showing a reverse plasticity mechanism, and the load case E shows a strong ratcheting mechanism, with the plastic strain increasing at every cycle. This directly confirms the accuracy of the predicted LMM lower and upper bound ratchet limits.

Parametric studies were performed further involving holes with different diameters

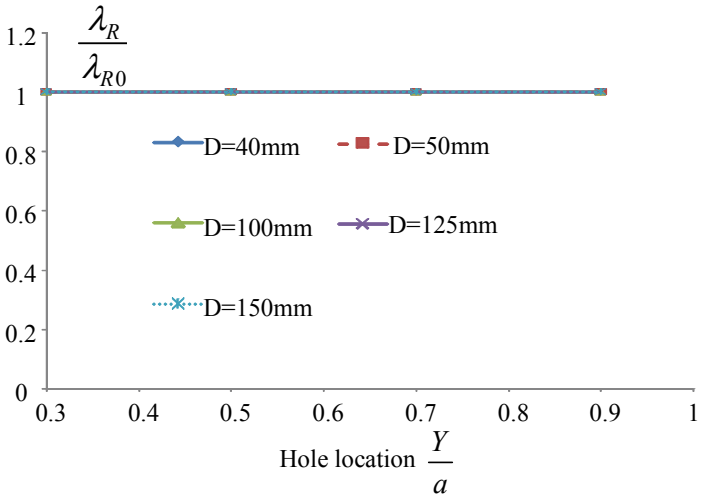

Figure 14: Variation of normalized ratchet limit multiplier with varying vertical hole location at fixed horizontal location $(X/a = -0.1)$ and prescribed reversed bending moment $(\Delta M/2)/\Delta M_0 = 1$

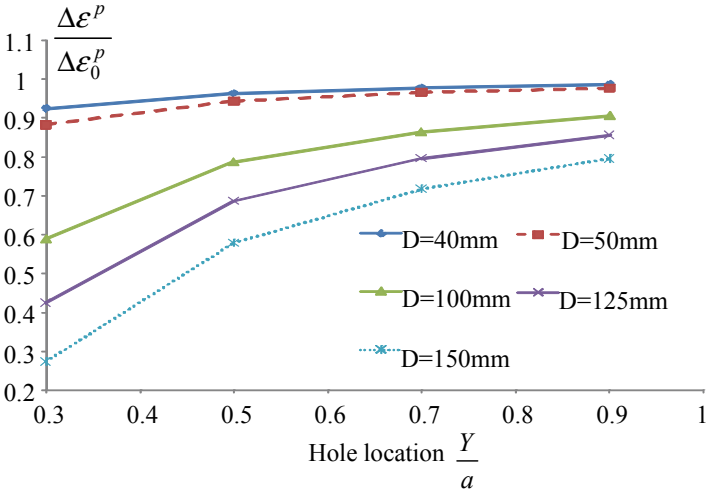

Figure 15: Variation of normalized maximum plastic strain range with varying vertical hole location at fixed horizontal location $(X/a = -0.1)$and prescribed reversed bending moment $(\Delta M/2)/\Delta M_0 = 1$

drilled at different locations. Figs.12 and 13 shows the variations of the ratchet limit and crack tip plastic strain range, respectively, due to the change of the horizontal hole location and diameter. It can be seen that for all diameter D, the optimum horizontal location where the maximum plastic strain range decreases the most with minimum effect on the ratchet limit is located at a distance 10% of the semi-cracked length from crack tip opposite the ligament, i.e. X/a=-0.1.

Figs.14 and 15 presents the variations of the ratchet limit and crack tip plastic strain range, respectively, due to the change of the vertical hole location and diameter. It is observed that for the fixed horizontal location ($X/a = -0.1$), the ratchet limit keeps unchanged for different vertical hole locations and diameters, but the crack tip plastic strain range varies significantly with the change of vertical hole location and diameter. Hence the most significant decrease in crack tip plastic strain range with least reduction in the ratchet limit is identified for the hole size D=150mm at the optimum location $X_0/a = -0.1$, $Y_0/a = 0.3$, which gives a 72% reduction in the plastic strain range and does not reduce the ratchet limit.

8 Conclusions

This paper concentrates on the behaviour of an elastic-perfectly plastic body subjected to cyclic loading. The design limits in plasticity including shakedown limit, ratchet limit, plastic strain range concerning fatigue crack initiation have been solved by characterizing the steady cyclic state using a general cyclic minimum theorem. For an approximating class of kinematically admissible strain rate histories, the minimum of the functional for these design limits are found by a simple programming method, the Linear Matching Method. Three practical examples of the LMM are provided to confirm the efficiency and effectiveness of the method and demonstrate that Direct Methods may be applied to a much wider range of circumstances than have hitherto been possible.

Acknowledgement: The author gratefully acknowledges the support of the Engineering and Physical Sciences Research Council (EP/G038880/1) of the United Kingdom, and the University of Strathclyde during the course of this work. The author would also like to thank Prof Alan Ponter of the Department of Engineering, Leicester University, for his advice and discussion on the theoretical development of the LMM.

References

ABAQUS. (2007): User's manual. Version 6.7.

Ainsworth R.A. (editor) (2003): An assessment Procedure for the High Tempera-

ture Response of Structures. R5 Issue 3, British Energy Generation Ltd.

Carter, P. (2005): Analysis of cyclic creep and rupture. Part 2: calculation of cyclic reference stresses and ratcheting interaction diagrams. *International Journal of Pressure Vessels and Piping,* vol. 82, Issue 1, pp. 27-33.

Chen, S.; Liu, Y.; Cen, Z. (2008): Lower bound shakedown analysis by using the element free Galerkin method and non-linear programming. *Computer Methods in Applied Mechanics and Engineering*, vol. 197, Issues 45-48, pp. 3911-3921.

Chen, H.F.; Ponter, A.R.S. (2001): A method for the evaluation of a ratchet limit and the amplitude of plastic strain for bodies subjected to cyclic loading. *European Journal of Mechanics - A/Solids*. vol. 20, pp. 555-571.

Chen, H.F. (2010): Lower and upper bound shakedown analysis of structures with temperature-dependent yield stress. *Journal of Pressure Vessel Technology*. vol. 132, pp.1-8.

Chen, H.F.; Ponter, A.R.S. (2010): A Direct Method on the Evaluation of Ratchet Limit. *Journal of Pressure Vessel Technology*. vol. 132, pp. 041202.

Chen, H.F.; Ponter, A.R.S; Ainsworth, R.A. (2006): The Linear Matching Method applied to the High Temperature Life Integrity of Structures, *International Journal of Pressure Vessels and Piping*, vol. 83(2), pp. 123-147.

Chen, H.F.; Ponter, A.R.S. (2005): Integrity assessment of a 3D tubeplate using the linear matching method. Part 1. Shakedown, reverse plasticity and ratchetting, *International Journal of Pressure Vessels and Piping*, vol. 82(2), pp. 85-94.

Koiter, W.T. (1960): General theorems for elastic plastic solids. Progress in solid mechanics, Vol.1, J.N.Sneddon and R.Hill, eds., North Holland, Amsterdam, pp. 167-221.

Mackenzie, D.; Boyle, J.T.; Hamilton, R. (2000): The elastic compensation method for limit and shakedown analysis: a review. Trans IMechE, *Journal of Strain Analysis for Engineering Design*. vol. 35, pp.171-188.

Maier, G. (1977): Mathematical programming methods for deformation analysis at plastic collapse. *Computers and Structures*, vol. 7, pp.599–612.

Marriott, D.L. (1998): Evaluation of deformation or load control of stresses under inelastic condition using elastic finite element stress analysis. *Proc. ASME Pressure Vessel and Piping conference*, Pittsburg, PA, PVP-136, pp. 3-9.

Melan, E. (1936): Theorie Statisch Unbestimmter Systeme aus Ideal-Plastischem Bastoff. Sitzungsberichte der Akademie der Wissenschaft, Wien, Abtiia. Vol. 145, pp. 195–218.

Nguyen-Tajan, T.M.L.; Pommier, B.; Maitournam, H.; Houari, M.; Verger, L.; Du, Z.Z.; Snyman, M. (2003): Determination of the stabilized response of

a structure undergoing cyclic thermal-mechanical loads by a direct cyclic method. *Abaqus Users' Conference Proceedings.*

Ponter, A.R.S; Chen, H.F. (2001): A minimum theorem for cyclic load in excess of shakedown, with application to the evaluation of a ratchet limit. *European Journal of Mechanics - A/Solids*. vol. 20, pp. 539-553.

Ponter, A.R.S.; Engelhardt, M. (2000): Shakedown limits for a general yield condition: implementation and examples for a von Mises yield condition, *European Journal of Mechanics, A/Solids*, vol. 19(3), pp. 423-446.

Seshadri, R. (1995): Inelastic Evaluation of Mechanical and Structural components Using the Generalized Local Stress Strain Method of Analysis. *Nucl. Eng. Des.* vol. 153, pp. 287-303.

Staat, M.; Heitzer, M. (2001): LISA a European Project for FEM-based Limit and Shakedown Analysis. *Nuclear Engineering and Design*, vol. 206, pp. 151–166.